

Thesis Synopsis

Name of the student: Dipali Sonawane

Department: Materials Engineering, Indian Institute of Science, Bangalore-560012

Title of the thesis: Mechanical Reliability of Metal-Si Systems at different Length scales under Thermal Cyclic Loading

Metal structures of nanometer to micrometer sizes in different configurations, such as thin films, thick coatings and 3D interconnects, are widely used for conducting electrical signals in several semiconductor-based devices, such as microelectronic chips, photovoltaics (PV), micro/nano-electromechanical systems (MEMS/NEMS) etc. In practice, the main challenge that confronts the structural reliability of these systems arises due to the wide difference in the coefficient of thermal expansion (CTE) of metal (Cu: $17.5 \times 10^{-6} \text{ K}^{-1}$, Ag: $19 \times 10^{-6} \text{ K}^{-1}$, Al: $23 \times 10^{-6} \text{ K}^{-1}$) and Si ($2.7 \times 10^{-6} \text{ K}^{-1}$); This generates large thermal stresses during fabrication, post-fabrication annealing as well as thermal excursions during service. Thus, it is necessary to engineer the devices based on the understanding of the microscopic processes that lead to deformation and failure of these structures under cyclic thermal stresses to ensure their reliable functioning over the designed service life. In this regard, three metal-Si systems, namely Cu filled through Si vias (TSV), PV solar cell and thin metal film/particles on Si - all having different geometrical constraints as well as characteristic length-scales-were investigated in the course of this work.

The first metal-Si system studied was 100 μm diameter Cu- filled TSV (Cu-TSV) which are used as the interconnects in the 3D microelectronic systems. In this segment of the study, the effect of TSV fabrication process and subsequent annealing (temperature range of 250 to 550 $^{\circ}\text{C}$) and accelerated thermal cycling (temperature range of -50 to 150 $^{\circ}\text{C}$) on its structural integrity was studied. During annealing and thermal cycling tests, grain boundary sliding

induced non-uniform extrusion of Cu (see **Fig. 1a** and **1b**), Cu-Si reaction and nucleation of micro-cracks in Si (see **Fig. 1c**) were observed, whereas during post-annealing ageing at room temperature, slow growth of the micro-cracks in Si was observed. Electron back-scatter diffraction (EBSD) analysis of extruded grains and crystal plasticity (CP) simulations indicated only a minor role of elastic-plastic anisotropy in the non-uniform extrusion of Cu. The micro-crack nucleation in Si was observed as a result of the residual thermal stresses and the volumetric stress associated with the Cu-Si compound formation. The conclusion was supplemented by stress measurement using Raman spectroscopy. Subsequently, slow crack growth observed in Si was attributed to the oxidation of Si at the crack tip (see **Fig. 2**), which was confirmed by extended finite element method (XFEM) and contour integral based finite element analysis (FEA), electron-probe micro-analysis (EPMA) and ageing of Cu-TSV samples inside high vacuum environment.

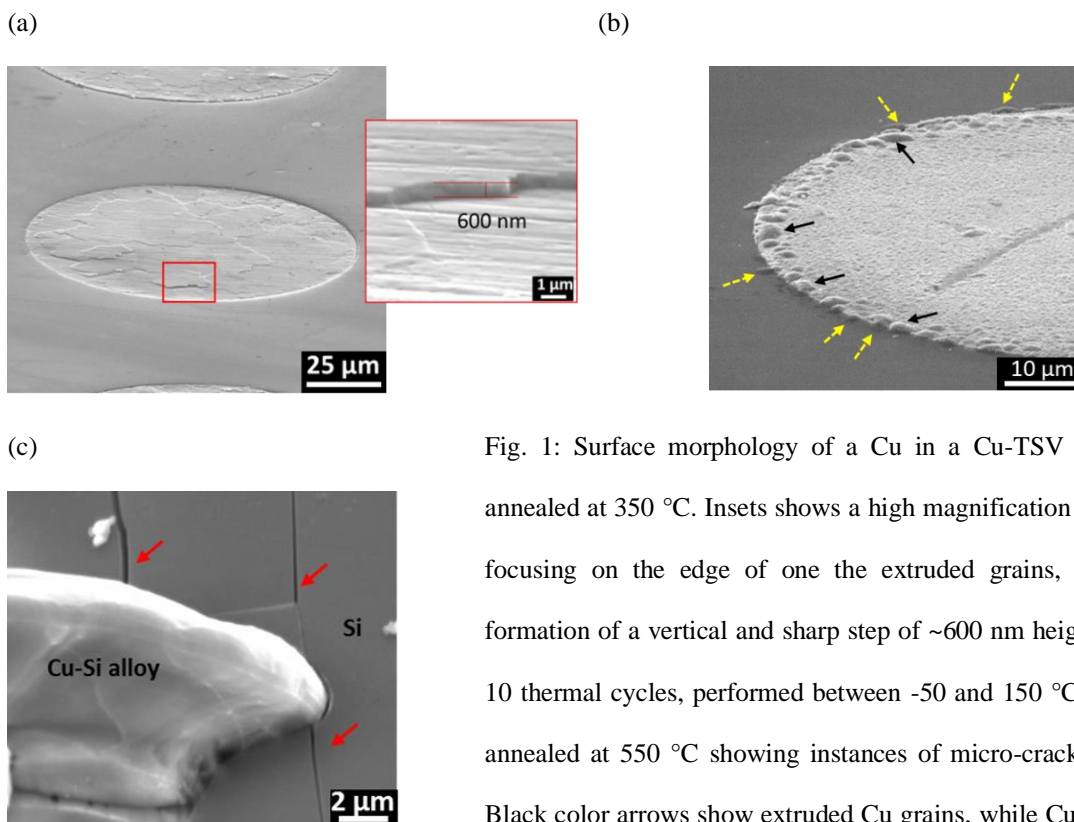


Fig. 1: Surface morphology of a Cu in a Cu-TSV sample: (a) annealed at 350 °C. Inset shows a high magnification micrograph focusing on the edge of one of the extruded grains, revealing a formation of a vertical and sharp step of ~600 nm height. (b) after 10 thermal cycles, performed between -50 and 150 °C (c) sample annealed at 550 °C showing instances of micro-crack formation. Black color arrows show extruded Cu grains, while Cu-Si reaction occurrence sites and micro-cracks are shown with yellow and red color arrows respectively.

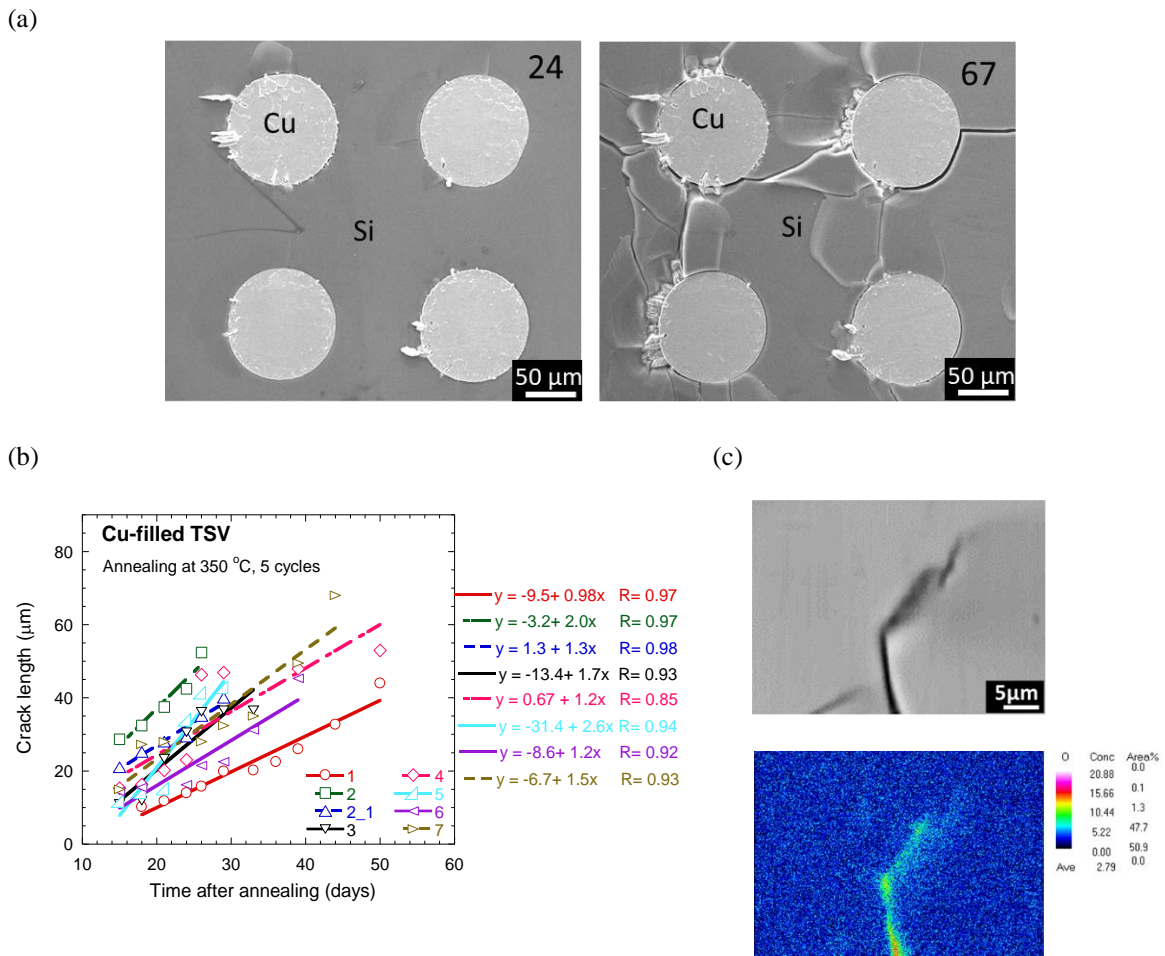


Fig. 2: (a) SEM micrographs showing the growth of numerous cracks in an array of Cu-TSV during natural ageing at room temperature. The number written on the top-right corner of each micrograph represents the day since the annealing treatment at 350 °C. (b) Variation of crack length of different surface cracks with the duration of natural ageing. The symbols show the actual datum point, whereas the straight lines are the best linear curve-fits, whose equations, along with values of the regression parameter (R), are given in the legend. (c) SEM micrograph and corresponding elemental mapping, performed using EPMA, of oxygen in a region in Si wafer comprising of a crack growing during natural ageing corresponding to the 27th day of natural ageing.

The second system studied was commercial PV solar cell, which has flat metal coatings of a few tens of micrometer thickness on both the top surface and the bottom or backside of Si. To assess mechanical reliability, accelerated thermal tests were carried out on the PV solar cell samples (temperature range of -40 to 90 °C and -50 to 150 °C) which showed that Ag-Si interface (i.e. on top) is less susceptible for cracking as compared to Al-Si interface present at bottom (see **Figs. 3a** and **3b**). Ideal geometry and microstructurally sensitive FEA showed that

plasticity in the Al-Si eutectic layer precluded deflection of the cracks into Si. Further, XFEM based analysis showed that the wavy interface was more susceptible to fracture as compared to the flat interface. This prediction was confirmed by performing thermal cycling tests on PV solar cell samples having a substantially less wavy interface between Al and Si, which showed improved resistance to crack nucleation and growth (see **Figs. 3c** and **3d**).

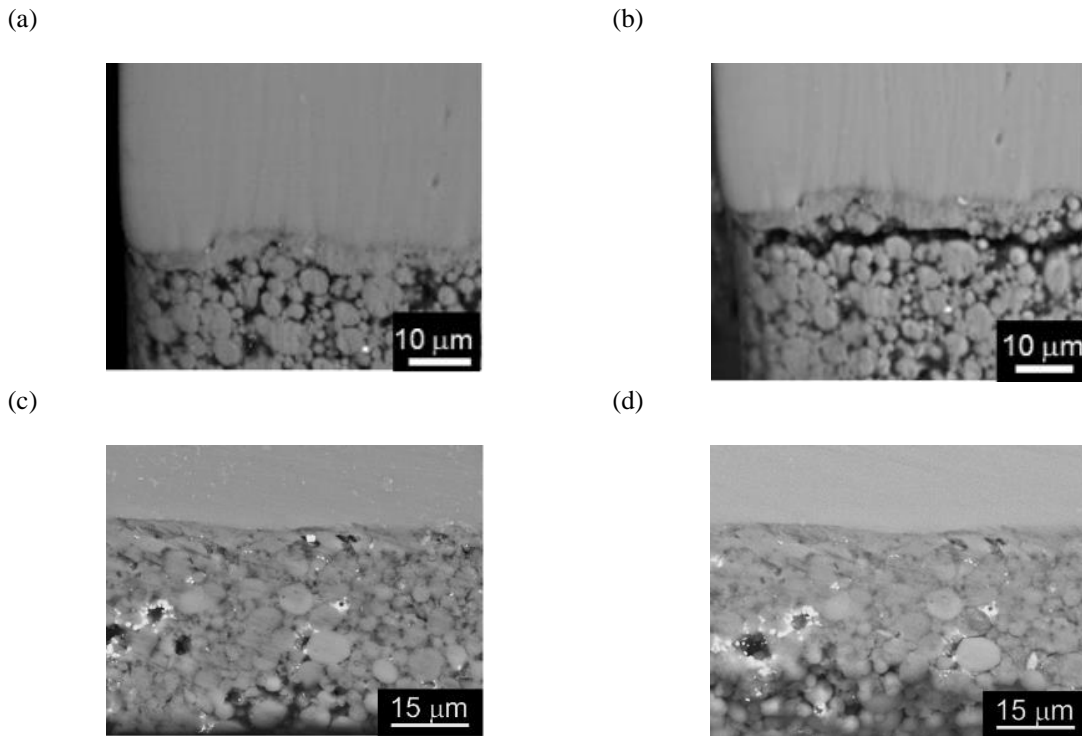


Fig. 3: SEM micrographs showing the cross-section of solar cell near the Al-Si interface: A sample with wavy interface (a) before and (b) after 5 thermal cycles. A sample with relatively smooth interface (c) before, (d) after 55 thermal cycles with no signs of delamination or micro-crack formation at the interface between eutectic and Al layer. Thermal cycling was performed between -40 and 90 °C, with ramp-rate 100 °C/h during heating and cooling segments.

The third metal-Si system studied in the work was Cu nano- and micrometer sized particles on the Si, which were formed via dewetting of 10 - 40 nm thick Cu films sputter deposited on Si. The kinetics of dewetting of Cu thin films, which was used to fabricate Cu particles on Si, was investigated using in-situ annealing experiments, carried out inside a scanning electron microscope (SEM) and phase-field modelling. It was observed that Cu

dewetting is governed by the void nucleation at triple points (see **Fig. 4a**) and the fractal growth of voids (see **Fig. 4b**) through surface diffusion mechanism (see **Figs. 4c** and **4d**).

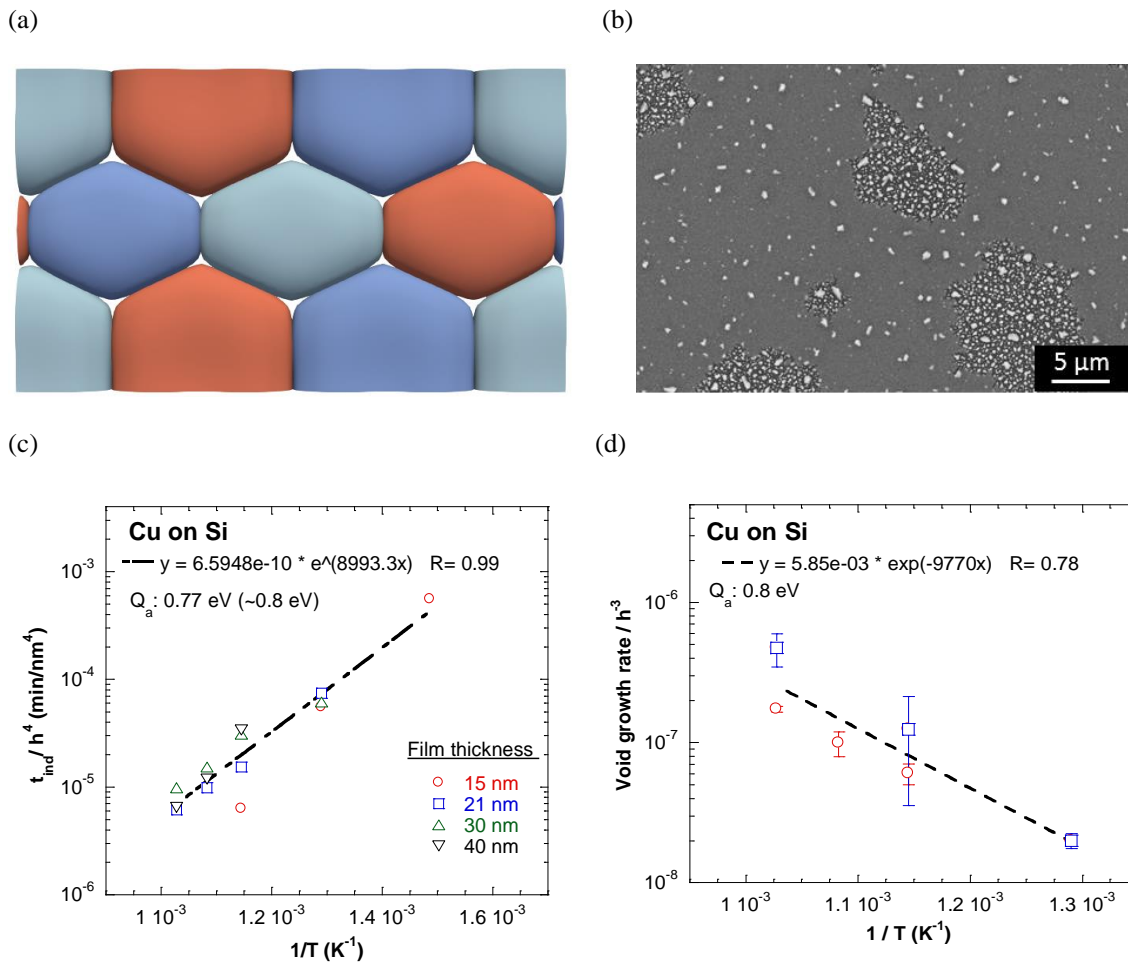


Fig. 4: (a) Contour plot showing the void nucleation at quadruple points during initial stages of dewetting as obtained from phase-field simulations (b) dewetting of Cu film on Si through growth of the void fractals. (c) Variation of normalized induction time required for the void nucleation (i.e., t_{ind}/h^4) as a function of $1/T$ and (d) variation of growth rate of the fractal voids normalized by dividing it with inverse cube of the film thickness as a function of inverse of the absolute temperature. In each graph, symbols show experimental datum points, whereas straight lines show the best curve-fits. Equation for the best curve-fits, along with the regression parameter, R , are given in each graph.

Subsequently, thermal cycling, annealing and shock tests were carried out on Cu nanoparticles-Si system using different heating-cooling ramp rates over the temperature range of -25 and 150 °C, and 25 and 400 °C. With faster rate, changes in shape and size of the Cu

particles and re-dewetting of the residual Cu layer were observed (see **Fig. 4a** and **4b**), while slow cooling rate did not induce any such effect, even if the annealing was performed at high temperature (e.g., 400 °C) (see **Fig. 4c** and **4d**). It is understood that the heating-cooling rate controls the deformation of Cu particles, which is highly sensitive to length scale as well as strain rate.

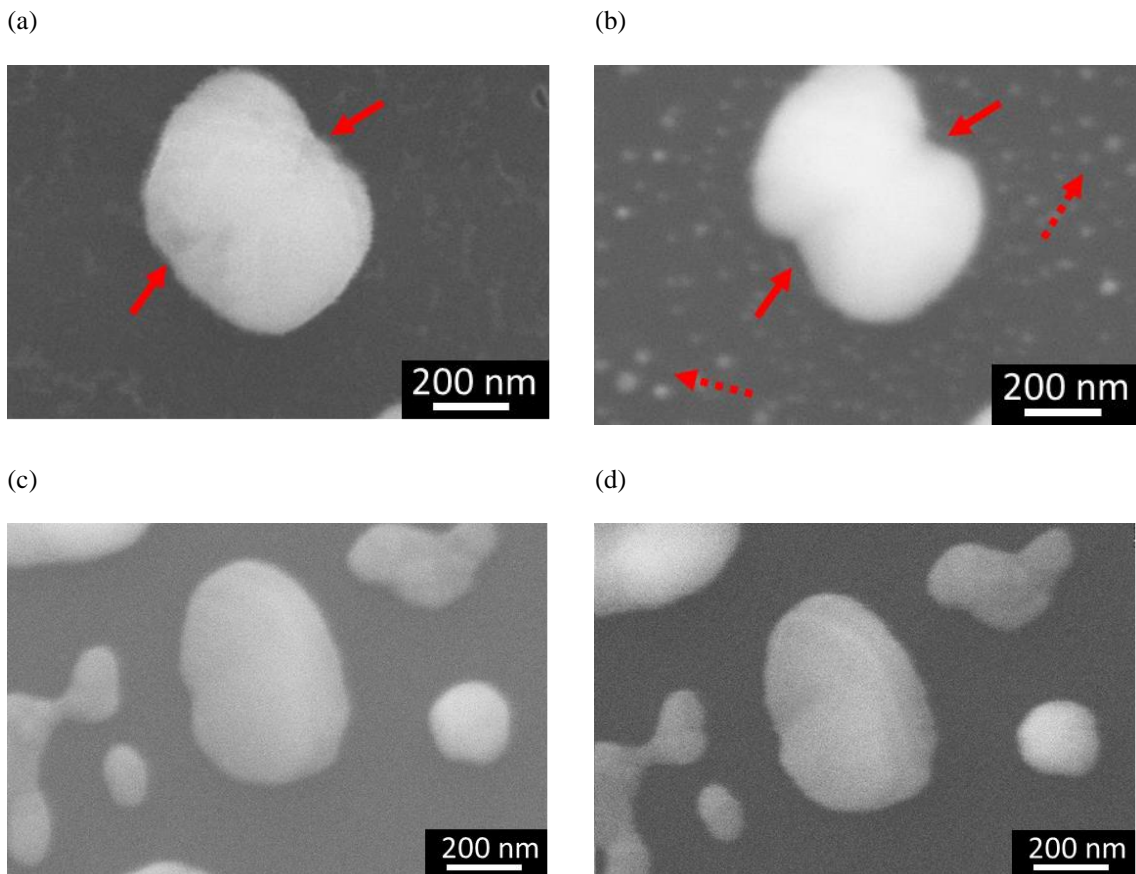


Fig. 5: SEM micrographs showing a set of Cu particles (c) before, and after (b) 15 thermal (shock) cycles with faster heating-cooling ramp rate. The thermal shock cycling was performed between 25 °C and 400 °C; the dwell times at the highest and the lowest temperatures were 5 and 1 min, respectively. Arrows indicate the locations where shrinkage in the particle size was evident and re-dewetting of residual Cu layer took place. (c) Before and (d) after 10 thermal cycles with a 10 minutes dwell at the maximum temperature. The thermal cycling was performed in the temperature range of 25 to 400 °C with a heating ramp rate 0.02 °C/s and furnace cooling.

In conclusion, the study performed on different systems revealed a strong effect of length scales and metal-Si boundary conditions (due to geometric constraints) on the structural

integrity of metal-Si systems. The difference in the geometry and length scale of these systems resulted in a specific type of failure phenomena in each system, even when they were subjected to a similar type of thermal excursions. For example, thin metal structures required high strain rate (i.e. heating-cooling ramp rate) or a greater number of annealing/thermal cycling for noticeable deformation or final failure to occur. Cu-TSV system was observed to be less prone to Cu extrusion when subjected to thermal cycling with fast ramp rate, whereas slow heating cooling rate resulted in enhanced extrusion of Cu (i.e., time dependent deformation of Cu). Besides, the increased number of annealing cycles led to the failure of interlayer (diffusion barrier layer) deposited between Si and metal (Cu), leading to the Cu-Si reaction and subsequently crack nucleation in Si. Environmental factors, such as moisture and oxygen, were noted to be important parameters in controlling the final fracture of the Si in Cu-TSV system. In contrast, a solar cell where 25 to 35 μm Ag and Al coatings were present in planar geometry form on either side of Si, showed crack nucleation at the interface of eutectic layer-Al after first thermal cycle itself without showing noticeable permanent deformation in Al or Ag metal layer. On the other hand, a ductile eutectic layer of Al and Si, present at the interface between Al and Si, remained stable over the number of thermal cycles and shielded Si from cracking. Moreover, when metal layer dimension reduced to nanometer (or few micrometers) scale, annealing or thermal cycling caused a transition in final failure from cracking or delamination to the morphological changes, such as agglomeration of the metal layer or shrinkage in particle size over the substrate. These observations also suggest that probability of failure of Si in all three metal-Si systems decreased with reduction in the applied geometrical constraint applied (3D constraint in TSV versus 2D or 1D constraint in solar cell and Cu films) by metal filler or layer. The distinct transition in the thermal stress relaxation mechanism was observed in the metal-Si systems with reduction in the size of metal layers in contact with Si, e.g. in Cu-TSV system, plasticity and grain boundary sliding driven deformation of the Cu was major stress

relaxation mechanism, which was observed to be less dominant in the Al or Ag coatings in solar cell and Cu-thin films on Si. At smaller length scale, elastic stress relaxation through grain boundary grooving, voiding, hillock formation and shape evolution played a dominant role. On the other hand, the role of the microstructural features, such as crystallographic texture or particle size, in the deformation process was observed to be increasing from thicker to thinner structures of the metal layer, e.g. orientation of Cu grains (i.e., Cu anisotropy) in Cu-TSV system showed negligible effect on the Cu extrusion behavior or Si cracking, whereas it was an important factor in the agglomeration kinetics of Cu thin films during dewetting to enable grain boundary grooving driven void nucleation at the high angle grain boundaries usually present in the textured thin films. Further, it was observed that more homogenous (less porous) compact Al layer (which will need small size particles in Al layer) will be important to avoid the crack nucleation or delamination at the Al-eutectic interface in the solar cell. While in the case of Cu particles, smaller Cu particles (few nanometer size) showed shrinkage in their size and hence enhanced the morphological changes when subjected to thermal cycling.

In addition to above observations, it was inferred that structural reliability of a metal-Si system is also dependent on the processing routes employed during fabrication of metal-Si system, e.g. although rough sidewalls avoided interfacial sliding of Cu by providing mechanical friction, it can also act as a stress concentrator and damage nucleation sites during cyclic thermal loading conditions. In a solar cell system, interface waviness at the eutectic and Al interface was the reason for the stress concentration and hence for crack nucleation. For thin film system, surface roughness of the substrate will lead to curvature difference on the film surface, which will result in the less barrier for dewetting of thin films. These observations clearly suggest that irrespective of the length scale of the metal-Si system, the smooth interface at metal-Si contact is necessary to avoid the stress concentration. Furthermore, an effective

adhesion layer should be deposited between metal and Si to avoid delamination or voiding in the metal layers deposited on Si during early stages of thermal excursions.

Nevertheless, the study performed on different systems revealed a strong effect of length scale, metal-Si boundary conditions and processes involved in the fabrication on the structural integrity of the metal-Si systems. It is strongly suggested that for correctly ascertaining the response of a metal-Si system, studies specific to the length-scale, geometry and the boundary condition must be undertaken and any sort of extrapolation as well as interpolation must be avoided.